Synthesis, Microstructure, and Mechanical Properties of Aluminum/Granulated-Slag Composites

A. Torres, J. Cruz, L. Hernández, L. Ma. Flores-Vélez, and O. Domínguez

(Submitted 22 January 2001; in revised form 9 May 2001)

The present work provides results of aluminum metal matrix composites reinforced with granulated slag (GS). The study concerns the synthesis and properties of Al/GS composites based on powder metallurgy techniques. Dilatometry, differential thermal analysis, and scanning electron microscopy were employed to track the reactions between the aluminum matrix and the granulated slag during the sintering treatment. Thermal analysis results revealed an exothermic reaction at 640 °C, leading to the formation of the intermetallic compound Al_3Fe. The hardness and compressive strength of the sintering compacts were determined as a function of the GS content. The best results were achieved with the aluminum composites with 15 wt.% GS, reaching compressive strengths up to 372 MPa.

Keywords aluminum metal composite, granulated slag reinforcement, mechanical properties, metal matrix composite

1. Introduction

At present, metal matrix composites (MMCs) have been developed to the level of commercial production. Nevertheless, the high cost of many of the reinforcing compounds remains the major barrier in the widespread use of composites in other applications. A possible way to avoid this handicap would be the employment of particles obtained from the recycling of some industrial solid wastes. The idea is becoming popular and several studies have been done with fly-ash, glass, and other by-products.[1,2]

Slag is one of the major waste products of steelmaking production, regularly generated each year in significant volumes as thousands of tons. This by-product has the potential for added value if a diversity of suitable end products could be produced from these materials. Tighter environmental regulations have prompted industry to search for new methods of treating their waste by-products. Because of the large quantities of slag produced in the manufacture of steel and the present expensive manner in which it is discarded, new methods for treating and using these solid wastes are required. The use of these solid wastes as reinforcing particles in metallic matrix is proposed among the possible applications of granulated slag (GS). The present work reports results concerning the manufacture and mechanical properties of Al/GS composites, which have the potential of becoming low-cost MMC materials.

A. Torres, J. Cruz, L. Hernández, and **O. Domínguez,** Departamento de Materiales, Instituto de Metalurgia-UASLP, 550 Sierra Leona CP 78210, San Luis Potosí, SLP/México; and **L. Ma. Flores-Vélez,** Laboratorio de QuÍmica Ambiental, Facultad de Ciencias Químicas-UASLP, 6 Dr. Salvador Nava CP 78210, San Luis Potosí, SLP/México. Contact e-mail: lflores@uaslp.mx.

2. Experimental Procedure

Commercially pure (99%) aluminum needles supplied by Sigma-Aldrich (Aceros San Luis Corp., San Luis Potosí, Mexico) were used in this investigation. Slag was received from a domestic steelmaking industry. Aluminum needles and slag were mechanically grounded using a ball-milling drum and subsequently mixed using a rotating drum blender. Hexane was incorporated during the aluminum milling process in order to reduce oxidation.

The phases and chemical compositions of the aluminum and slag were determined by x-ray diffraction (XRD) and energy dispersive x-ray spectroscopy (EDX). The final mean size of Al particles was 55 μm having a flake-like morphology (Fig. 1), and the slag particles presented an irregular morphology with a mean size of 35 μm (Fig. 2a). X-ray diffraction patterns indicated that the major components in the GS were CaO, SiO_2, and Fe_2O_3, with minor amounts of Al_2O_3 and MnO (Fig. 2b). Using a conventional pycnometer, a mean apparent density of 3.2 $g \cdot cm^{-3}$ was found for the slag once it was granulated.

Al/GS composites were manufactured using conventional powder metallurgy techniques such as uniaxial compaction and sintering. The powder mixtures were consolidated in air at room temperature of pressures ranging from 150 to 600 MPa, and the green density of compacts was determined by pycnometry as a function of the compacting pressure and GS composition. Table 1 shows the different Al/GS powder mixtures that were compacted and then sintered in Ar atmospheres up to 620 °C, in all cases using a heating rate of 10 °C/min, and at the final temperature employing different soaking times ranging from 0 to 1 h. Densification during sintering of green compacts was also evaluated as a function of increasing slag content using dilatometric techniques. Chemical reactions between Al and GS were tracked using differential thermal analysis (DTA). Finally, the hardness and compressive strength of the sintering compacts were determined to evaluate the mechanical properties of the composite material as a function of the GS content. Compressive tests were performed under displacement control using an Instrom (Instrom Limited, High Wycombe, U.K.) 20 kN screw-driven machine and a series of five cylindrical-

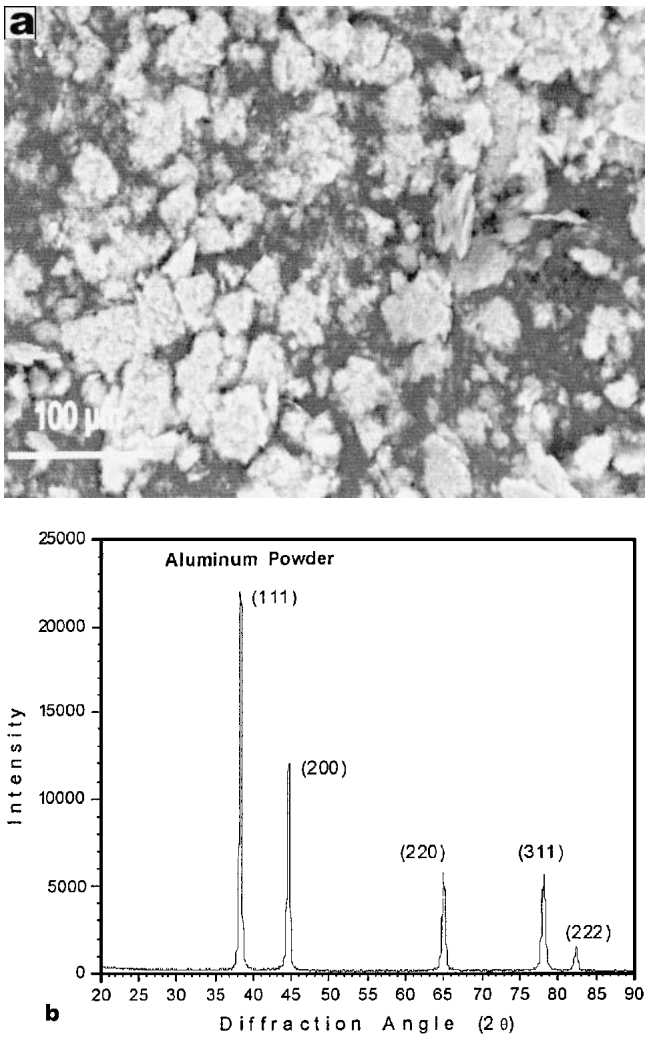

Fig. 1 (a) Scanning electron micrography and (b) x-ray diffraction pattern of aluminum powder

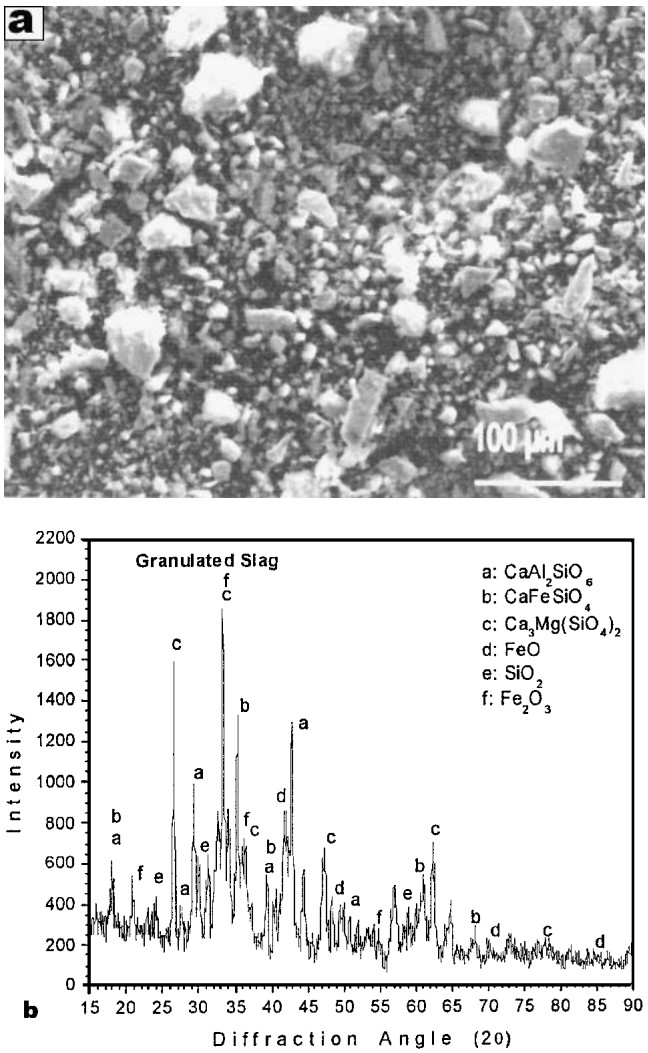

Fig. 2 (a) Scanning electron micrography and (b) x-ray diffraction pattern of as-prepared GS

shaped specimens of each blend were used with a diameter of 4 mm and a length of 8 mm, using a constant cross-head speed of 0.76 mm · min^{-1}.

3. Results and Discussion

The predominant goal in powder compaction is to achieve good compact properties with minimal applied force. Particle packing is important in powder forming processes, because the packing density determines the die fill, binder content, and shrinkage in sintering. Increasing pressure during compaction provides better packing (via particle rearrangement and plastic deformation) and leads to decreasing porosity with the formation of new particle contacts.[3] Powder metallurgy manufacturing experience has shown that green density of compacts depends on several parameters, such as particle morphology, chemical composition, surface area, mean particle size, and particle size distribution. Green density usually decreases with decreasing particle size, and densification of metallic powders is always easier than the densification of the powder mixtures.[4]

Table 1 Chemical Composition (wt.%) of the Prepared Composites

Designation	Aluminum	Granulated Slag
95A15GS	95	5
85A115GS	85	15
75A125GS	75	25
65A135GS	65	35

Figure 3 shows the effect of compaction pressure on Al powders, indicating that the sample density augment with increasing pressure approached relative densities of 98% at 600 MPa. Equivalent procedures were carried out with the different mixtures of Al and GS, observing on the Al/GS case that the presence of the slag particles inhibited densification (Fig. 3), achieving a density of only 90% in the 85Al15GS material produced at highest compaction pressure. Increasing the pres-

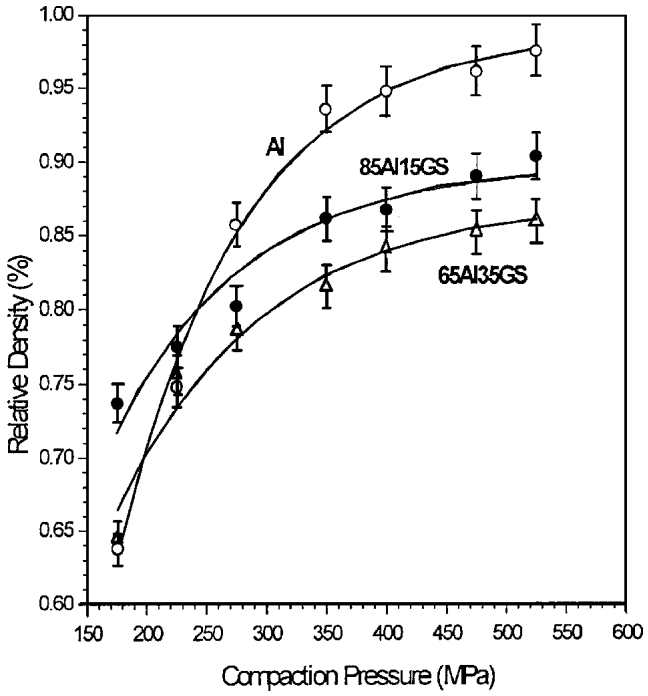

Fig. 3 Relative density versus compaction pressure of samples during Al and Al/GS powder consolidation

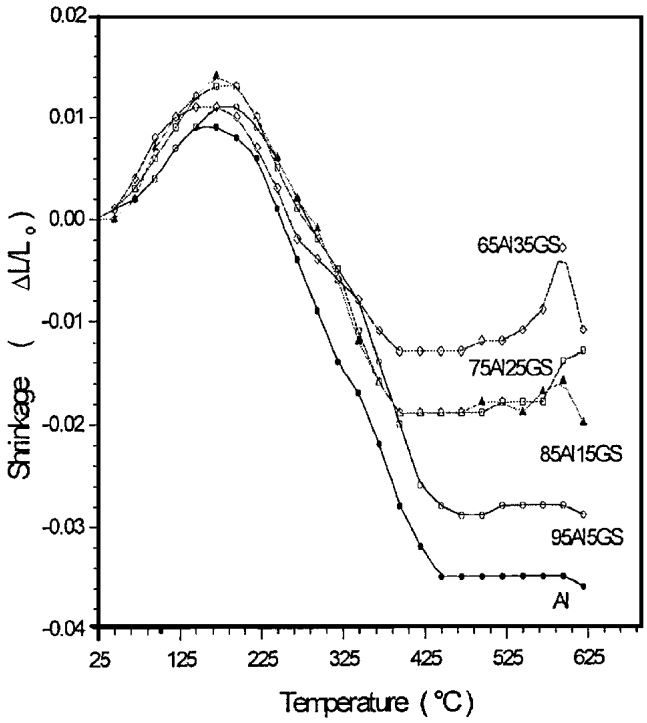

Fig. 4 Sintering curves of the Al/GS composites as a function of slag content. All samples compacted to 400 MPa.

ence of ceramic particles from 15 to 25 wt.% inhibited densification even more, obtaining a relative density of only 85% in the 65Al35GS material at the highest pressure and illustrating the problems usually associated with the MMC materials produced by powder metallurgy techniques (Fig. 3). In all cases, bulk density of composites was calculated according to the rule-of-mixture,[5] where the relative density corresponds to the ratio between compact density and theoretical density. In addition, the present results indicate that above 400 Mpa, the gain in densification in Al/GS compacts was quite small, hence all of the samples before sintering were compacted at this pressure.

During dilatometry, the experiments were carried out at a constant heating rate of 10 °C/min and relative shrinkage ($\Delta L/L_o$) was calculated as the change in sample length divided by its initial length. Figure 4 shows results obtained by dilatometry from samples having different GS content, and in all cases it was observed that shrinkage in Al/GS composites starts at 175 °C. After sintering the samples to 620 °C, the compact density measured at room temperature changes from 93 to 98% for pure Al, and from 86 to 90% for 85Al15GS, indicating that the final density of compacts during the sintering treatment is affected by the slag content on the sample, especially once the GS content exceeds 25 wt.%. In addition, the presence of peaks on the dilatometric curves at 600 °C (Fig. 4) could indicate not only a difference of thermal expansion coefficients between the matrix and the particles, but also the presence of other phenomena such as phase changes, release of trapped gas, oxidation, etc.

On the basis of thermodynamic considerations, there is the possibility of chemical reactions between the aluminum powder and the constituents of the GS such as SiO_2, Fe_2O_3, and Fe. In sufficient quantity, certain alloying elements can form intermetallic compounds with the aluminum and appear as second phase precipitates in the samples. Such interfacial reactions between the metal and the reinforcement particles would influence the properties of the composite. The possible chemical reactions between the aluminum powder and the constituents of the GS used in this study are shown as follows:[6]

$$3/2\ CaO(s) + Al(s) = 1/2\ Al_2O_3(s) + 3/2\ Ca(s)$$
$$\Delta G^0(893\ K) = 389.7\ kJ/mol \quad \text{(Eq 1)}$$

$$3/4\ SiO_2(s) + Al(s) = 1/2\ Al_2O_3(s) + 3/4\ Si(s)$$
$$\Delta G^0(893\ K) = -136.4\ kJ/mol \quad \text{(Eq 2)}$$

$$1/2\ Fe_2O_3(s) + Al(s) = 1/2\ Al_2O_3(s) + Fe(s)$$
$$\Delta G^0(893\ K) = -404.7\ kJ/mol \quad \text{(Eq 3)}$$

where the Gibbs free energy changes were calculated at 620 °C. In addition, according to the Al-Fe phase diagram, there is associated the formation of the Al_3Fe intermetallic compound as a product of the reaction:[7]

$$1/3\ Fe(s) + Al(s) = 1/3\ Al_3Fe(s) \qquad \Delta G^0(893\ K) = -75.6\ kJ \quad \text{(Eq 4)}$$

where the Gibbs free energy change in this chemical reaction was calculated using rough approximations.[6,8] At the sintering temperature (620 °C), the Gibbs free energy changes of the

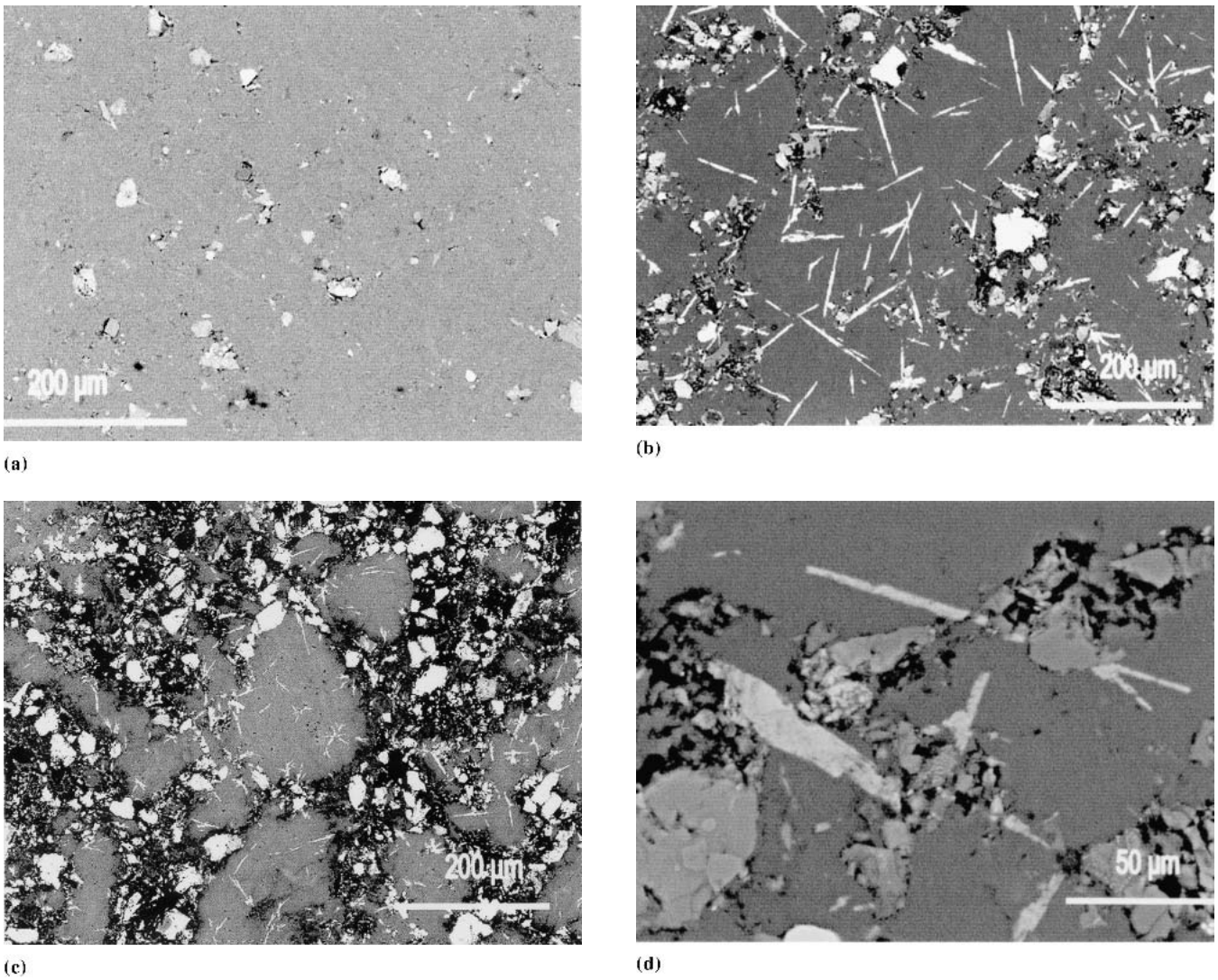

Fig. 5 Scanning electron micrographs showing typical microstructures in Al/GS composites sintered for 1 h at 620 °C. (a) 95Al5GS, (b) 85Al15GS, (c) 65Al35GS, and (d) enlargement of precipitates observed in 85Al15GS

chemical reactions in Eq 2, Eq 3, and Eq 4 are negative, indicating the possibility of chemical reactions between the aluminum powder and the reinforcement particles. Nevertheless, Gibbs free energy changes can only tell if reactions are plausible, and only the kinetics of the solid-state reactions will dictate the occurrence of such processes.

With the intention of assisting the densification of MMC blends and observing the possible occurrence of reactions during sintering, different soaking times at 620 °C were employed, attaining the best results with a thermal treatment of 1 h at this temperature. The corresponding scanning electron microscope (SEM) images of Al/GS composites heated to 620 °C and held for 1 h are shown in Fig. 5, where the typical microstructure of low GS content composite (95Al5GS) shows low porosity levels and relative uniform distribution of the GS (Fig. 5a). Nevertheless, clustering of the particles was observed (Fig. 5c) in the microstructure together with porosity at high slag contents (65Al35GS). Once the slag content in the composite was high enough (greater than 5 wt.%), the presence of needle-like precipitates was observed together with the incorporated slag particles in 85Al15GS, 75Al25GS (not shown in Fig. 5), and 65Al35GS composites (Fig. 5b and c), with EDX chemical analysis suggesting an Al-Fe intermetallic compound (probably Al_3Fe was observed). In general, the slag from the steelmaking industry always contains small amounts of iron, so the peak observed on the dilatometric curves at 600 °C (Fig. 4) could be associated with the formation of the Al_3Fe intermetallic compound as a product of the solid-state reaction (4) between iron and aluminum.

To evaluate the possible solid-state chemical reactions involved during heat treatment of Al/GS composites, DTA was carried out on Al/Fe, Al/SiO_2, Al/Fe_2O_3, and Al/GS samples. During DTA, all experiments were carried out at a constant heating rate of 10 °C/min and the furnace chamber was filled with flowing argon at 20 ml/min. Figure 6(a) represents the DTA curve obtained with aluminum powder. During heating, an endothermic process at 125 °C coming from decomposition of the organic compound used to avoid oxidation was observed, then

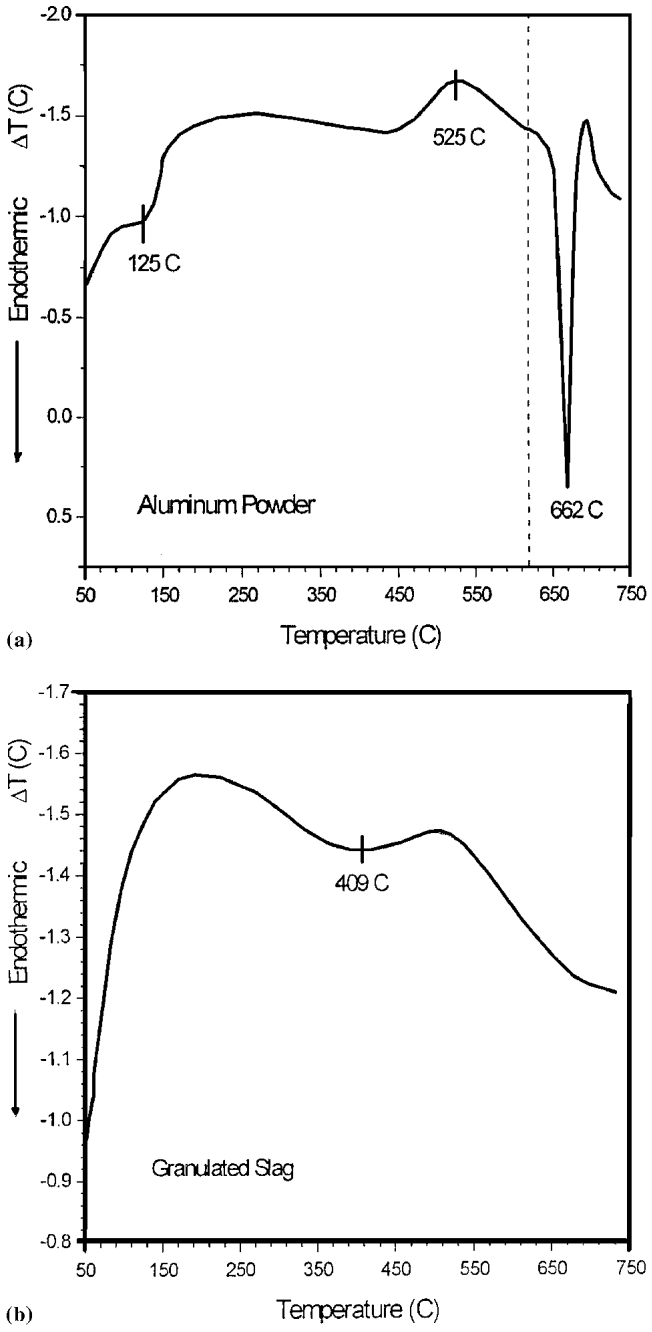

Fig. 6 DTA curves showing (a) hexane evaporation, grain growth, and melting in Al powder; (b) phase transformation in GS. The dotted line represents sintering temperature.

an exothermic peak at 525 °C assigned to grain growth during the sintering process was seen, and finally the characteristic endothermic peak at 662 °C associated with aluminum melting was observed. Figure 6(b) corresponds to the DTA curve obtained with GS powder, where an endothermic process not yet estimated was observed at 409 °C in the experimental temperature range. The DTA results concerning the reference samples Al/Fe, Al/SiO_2, and Al/Fe_2O_3 are presented in Fig. 7. Figure 7(a) and (b) corresponds to reactions in Eq 2 and Eq 3 and in both cases the presence of two well-defined exothermic peaks

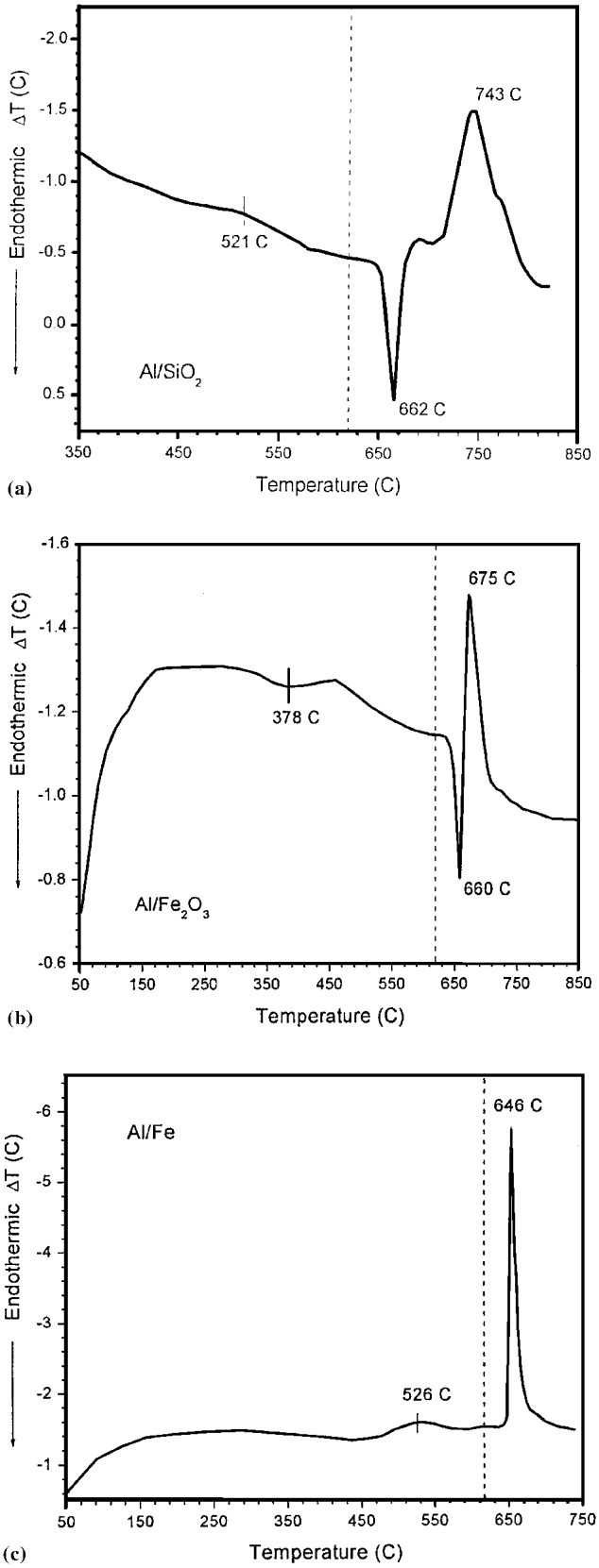

Fig. 7 DTA curves obtained from reference samples (a) Al/SiO_2, (b) Al/Fe_2O_3, and (c) Al/Fe. The dotted line represents sintering temperature.

above the melting point of Al were discerned: one at 743 °C and the other at 675 °C for Al/SiO_2 and Al/Fe_2O_3, respectively. On the other hand, the thermogram in Fig. 7(c) corresponding to sample Al/Fe clearly indicates the exothermic peak at 646 °C associated to the reaction in Eq 4, denoting that the Al_3Fe intermetallic compound can be obtained in the solid state. The formation of intermetallic compounds of Al in the solid state has been observed in other systems,[9] so the results indicate that this chemical reaction takes place well below the melting point of Al (662 °C).

Once the reference DTA curves were attained, the same procedure was carried out with Al/GS composites, and thermograms such as those shown in Fig. 8 were obtained. DTA curves obtained with the composites 95Al5GS and 85Al15GS especially reflect the different peaks appearing as a consequence of the slag content. According to Fig. 8(a), a low slag content was observed with the same phenomena as in pure Al and GS; i.e., first the decomposition of the organic compound at 125 °C, then the endothermic peak found in the slag at 409 °C, followed by grain growth during the sintering of aluminum at 525 °C, and finally the endothermic peak at 662 °C associated with the melting point of aluminum. Conversely, Fig. 8(b) indicates that at higher slag content, the thermogram presents the peaks mentioned before together with the presence of two exothermic peaks, determined at 640 and 694 °C. The first of these two peaks could be associated to the reaction in Eq 4 according to Fig. 7(c), whereas the second one is associated to reactions in Eq 2 and Eq 3, according to Fig. 7(a) and (b). These results suggest that the only reaction involved in the solid state during heat treatment of Al/GS composites concerns the Al_3Fe formation. Therefore, according to experimental results obtained by DTA, it is not likely that silica and iron oxides were reduced by aluminum powder in the solid state. In addition, EDX results were unable to detect the presence of silicon in the aluminum matrix.

Diffusive mass transport takes place when there is a gradient in the chemical potential and when the species in question has sufficient mobility. The diffusion coefficient of Fe in Al can be approximately estimated to 10^{-9} $cm^2 \cdot s^{-1}$ at 620 °C,[10] and those for the corresponding diffusion of the cationic species in the oxide lattice can be estimated in the range from 10^{-15} to 10^{-10} $cm^2 \cdot s^{-1}$ at the same temperature.[11] Because of the experimental conditions and according to diffusional information, if reduction takes place in the solid state, it should be in the metal-GS interface. There is experimental evidence indicating that there is progressive reduction of silica and iron oxide when processing for longer times at the melting temperature of aluminum.[12] Nevertheless, the results suggest that during the solid state sintering process, the fastest reaction concerns the interaction between metallic iron in the GS and Al powder forming the needle-like intermetallic precipitate observed on the Al/GS composites. At this stage, more studies will have to be undertaken, especially those dealing with the diffusional behavior of the interface Al/GS particles, in order to discern the kinetics of the possible chemical reactions involved during processing.

In powder metallurgy, it is widely accepted that all the mechanical properties, including strength, elastic modulus, fatigue life, and fracture toughness, depend on the final density of the sintered material.[3,13] Moreover, it is well established that the mechanical properties of particulate MMC are sensitive to the spatial distribution of reinforcing particles,[14,15] and clusters of particles have an adverse effect, especially on the ductility and fracture toughness. Figure 9 shows Vickers hardness as a function of the GS content, indicating that increasing the GS to about 15 wt.% can result in a considerable increase in the

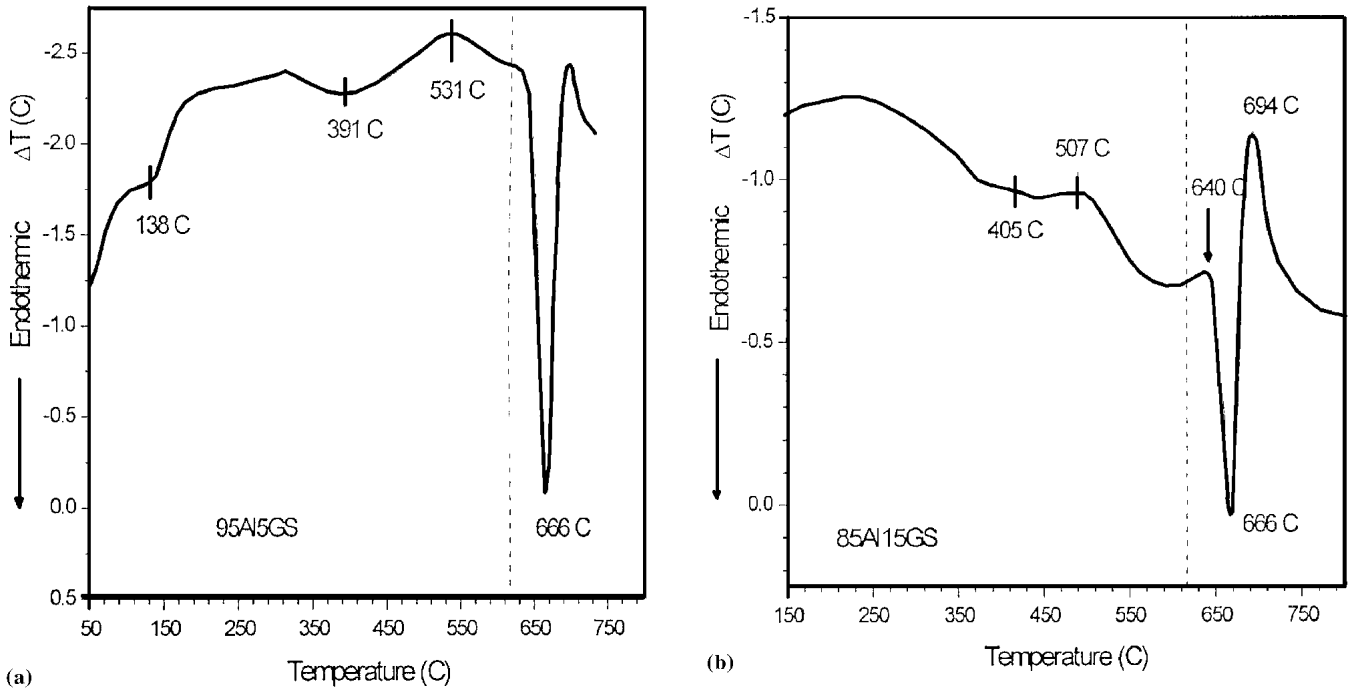

Fig. 8 DTA curves obtained from (a) 95Al5GS and (b) 85Al15GS. The dotted line represents sintering temperature.

MMC hardness, but beyond these limits, the slag particles weaken the material.

Regarding the mechanical response of the MMC, Fig. 10 shows the typical compression stress-strain curves of the Al/GS composites compacted at 400 MPa, then heated to 620 °C and held for 60 min. The compressive strength of the Al/GS composites (Fig. 10) is relatively high compared to the compressive strength obtained for pure Al (173 MPa). Following the hardness results (Fig. 9), the maximum compressive strength was obtained with a GS content corresponding to 15 wt.%.

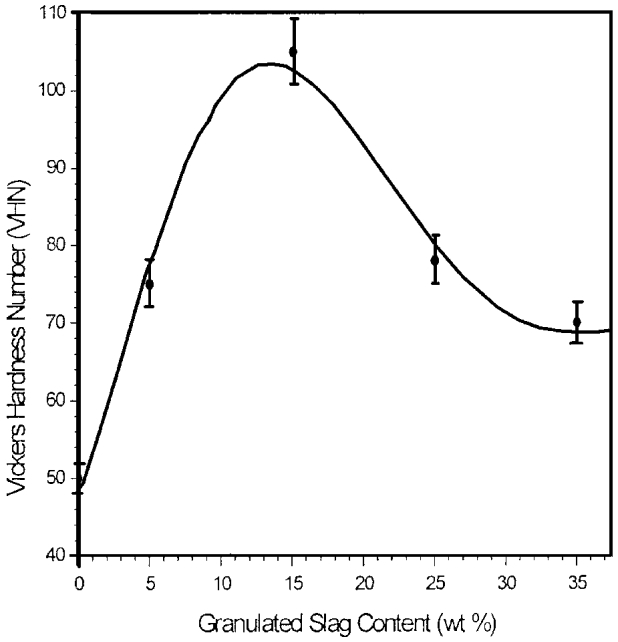

Fig. 9 Effect of the slag particle content on the Al/GS composite hardness. All samples were compacted at 400 MPa and sintered at 620 °C for 1 h.

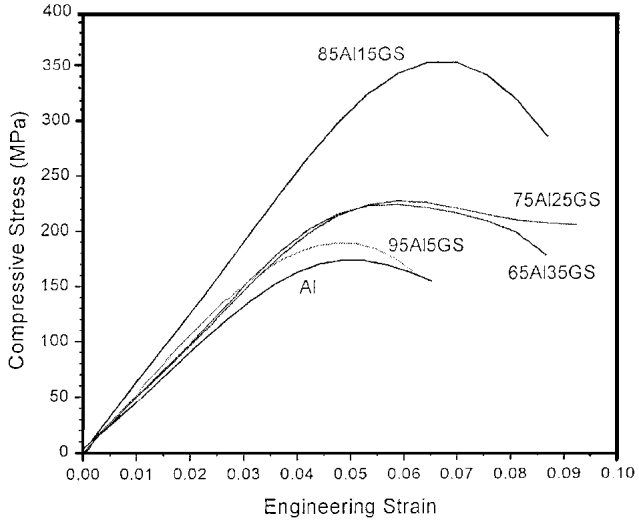

Fig. 10 Effect of the GS content on the compressive behavior of the sintered Al/GS composites. All samples were compacted at 400 MPa and sintered at 620 °C for 1 h.

The high compressive strength observed here could be an indication of good interfacial bonding between the slag particles and the aluminum matrix in Al/GS composites. Another reason for this compressive strength could be the presence of the Al-Fe intermetallic compound produced during the synthesis of the composite (Fig. 5). In the present case, the compressive strength of the MMC made with 15% GS reached a value of 372 MPa. The effect of the slag particles on the strength of MMC is shown in Fig. 11. This figure clearly indicates that under the present conditions, the addition of GS can increase the MMC's compressive strength. Even if the GS performance is quite good and the nature of the present discontinuous reinforcement seems to enable an improvement in mechanical properties over the unreinforced matrix, the challenge in the future will be to improve the engineering properties of discontinuously reinforced MMC via casting processing, making them valuable at a competitive cost compared to their unreinforced counterparts.

4. Conclusions

The present results indicate that MMC made of Al/GS can be prepared by pressing and sintering techniques involving conventional powder metallurgy processing. The green and sintered densities of the MMC here obtained were low, ranging from 2.9 to about 3.1 g cm^{-3}. The mechanical response of the Al/GS composites was determined in compression. The highest compressive strength of the MMC made with 15% GS was 372 MPa. EDX, and thermal and microstructural analysis, indicate the presence of a solid-state reaction between aluminum and GS forming the intermetallic compound Al_3Fe. The nature of

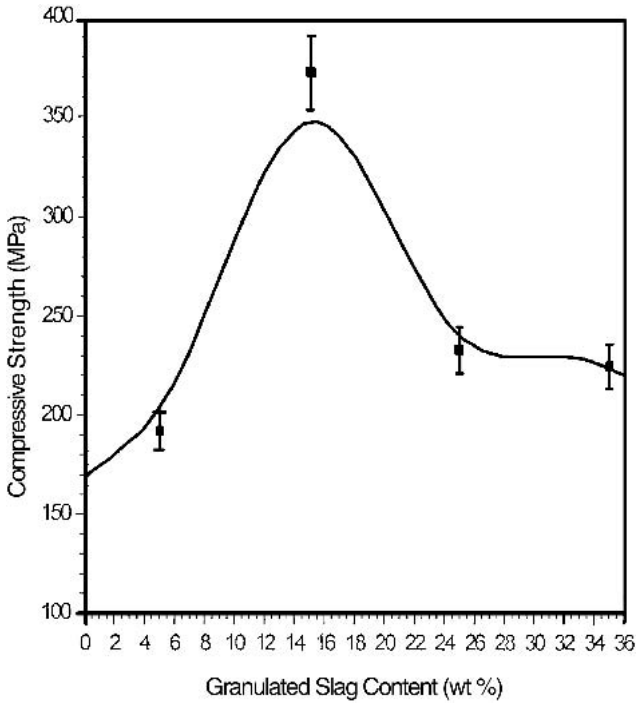

Fig. 11 Effect of GS content on the compressive strength of sintered compacts

the present discontinuous reinforcement seems to produce an improvement in mechanical properties over the unreinforced aluminum matrix.

Acknowledgment

Financial support provided by the SHIGO program (grant number 1998-02-05-006) is gratefully acknowledged.

References

1. P.K. Rohatgi, R.Q. Guo, P. Huang, and S. Ray: "Friction and Abrasion Resistance of Cast Aluminum Alloy-Fly Ash Composites," *Metall. Mater. Trans. A,* 1997, *28*, pp. 245-50.
2. L.M. Flores-Vélez, J. Chávez, L. Hernández, and O. Domínguez: "Characterization and Properties of Aluminium Composite Materials Prepared by Powder Metallurgy Techniques Using Ceramic Solid Wastes," *Mater. Manuf. Proc.,* 2001, *16*(1), pp. 1-16.
3. R.M. German: *Powder Metallurgy Science*, 2nd ed., Metal Powder Industries Federation, Princeton, NJ, 1994.
4. M.A. Meyers and K.K. Chawla: *Mechanical Behavior of Materials*, Prentice Hall, New York, 1999.
5. F. Delie and D. Bouvard: "Effect of Inclusion Morphology on the Densification of Powder Composites," *Acta Metall. Mater.,* 1998, *46*, pp. 3905-13.
6. O. Kubaschewski and C.B. Alcock: *Metallurgical Thermochemistry*, 5th ed., Pergamon Press Ltd., Oxford, England, 1979.
7. M. Hansen: *Constitution of Binary Alloys*, McGraw-Hill, New York, 1958.
8. R. Hultgren, R.L. Orr, P.D. Anderson, and K.K. Kelly: *Selected Values of Thermodynamic Properties of Metals and Alloys*, John Wiley, New York, 1963.
9. A. Bose: *Advances in Particulate Materials*, Butterworth-Heinemann, Newton, MA, 1995.
10. R.C. Weast and M.J. Astle: *CRC Handbook of Chemistry and Physics*, 63rd ed., CRC Press Inc., Boca Raton, FL, 1982.
11. Y.M. Chiang, D. Birnie, and W.D. Kingery: *Physical Ceramics*, John Wiley, New York, 1997.
12. R.Q. Guo and P.K. Rohatgi: "Chemical Reactions between Aluminum and Fly Ash during Synthesis and Reheating of Al-Fly Ash Composites," *Metall. Mater. Trans. B,* 1998, *29*, pp. 519-25.
13. R.M. German: *Sintering Theory and Practice*, John Wiley, New York, 1996.
14. A.M. Murphy, S.J. Howard, and T.W. Clyne: "Characterization of Severity of Particle Clustering and Its Effect on Fracture of Particulate MMCs," *Mater. Sci. Technol.,* 1998, *14*, pp. 959-68.
15. J.J. Lewandoski, C. Liu, and W.H. Hunt: "Effect of Matrix Microstructure and Particle Distribution on Fracture of an Aluminum Metal Matrix Composite," *Mater. Sci. Eng.,* 1989, *A107*, pp. 241-55.